Contents List available at VOLKSON PRESS

New Materials and Intelligent Manufacturing (NMIM)

DOI : http://doi.org/10.26480/icnmim.01.2018.101.103

Journal Homepage: https://topicsonchemeng.org.my/

ISBN: 978-1-948012-12-6

PHOTOLUMINESCENCE OF $(BA_{0.96}ND_{0.04})$ $(TI_{0.96}HO_{0.04})$ O_3 CERAMIC UNDER 638-NM EXCITATION

Dongxue Guan[1,2], Dayong Lu[1*], Xiuyun Sun[1]

[1]Key Laboratory for Special Functional Materials in Jilin Provincial Universities, Jilin Institute of Chemical Technology Chengde Street 45, Jilin 132022, China.

[2]College of Chemistry and Pharmaceutical Engineering, Jilin Institute of Chemical Technology, Chengde Street 45, Jilin 132022, China.

**Corresponding Author Email: dylu@jlict.edu.cn*

ARTICLE DETAILS

Article History:

Received 26 June 2018
Accepted 2 July 2018
Available online 1 August 2018

ABSTRACT

$(Ba_{0.96}Nd_{0.04})$ $(Ti_{0.96}Ho_{0.04})$ O_3 (BNTH4) ceramic with a cubic perovskite structure was prepared using the cold-pressing ceramic technique of solid-state reaction. Under 638-nm excitation, the photoluminescence (PL) monitoring provided the evidence of a small number of Ho^{3+} ions at Ba-sites. BNTH4 exhibits the multiplicity of PL signals of Nd^{3+} and Ho^{3+}. Ho^{3+} in BNTH4 exhibits an asymmetric amphoteric behavior, i.e., 3.82 at. % Ho^{3+} ions dominantly occupy Ti-sites and 0.18 at.% Ho^{3+} ions occupy Ba-sites.

KEYWORDS

Nd and Ho co-doped $BaTiO_3$ ceramic, X-ray diffraction, backscattered electron image, photoluminescence, site occupations

1. INTRODUCTION

Rare-earth-doped barium titanate ($BaTiO_3$) ceramics with a perovskite structure are widely applied in multilayer ceramic capacitors (MLCC) [1]. When double rare earths are used as co-dopants in $BaTiO_3$, most researches focused on the up-conversion luminescence, the energy transfer between two rare-earth ions, and core-shell-structured $BaTiO_3$ ceramics prepared at lower sintering temperatures ($T_s \leq 1300$ °C) [2–11].

Neodymium (Nd) and holmium (Ho) in $BaTiO_3$ were all reported to exhibit a photoluminescence (PL) behavior [12-16]. PL of Nd/Ho co-doped $BaTiO_3$ was reported under 532-nm laser over the last few mouths [17]. However, no investigation was reported about PL of this kind of ceramic under different laser wavelengths.

In this work, a Nd/Ho co-doped $BaTiO_3$ ceramic was investigated using 638-nm laser excitation. The multiplicity of PL signals of Nd^{3+}/Ho^{3+} was reported.

2. EXPERIMENTAL

Raw materials were reagent-grade $BaCO_3$, TiO_2, Nd_2O_3, and Ho_2O_3 powders. The ceramics was prepared according to the nominal compositions $(Ba_{0.96}Nd_{0.04})(Ti_{0.96}Ho_{0.04})O_3$ (BNTH4) using the cold-pressing ceramic technique of solid-state reaction method, as described elsewhere, The final sintering condition was T_s = 1400 °C for 12 h in air [17].

Powder X-ray diffraction (XRD) measurements were performed between 20° ≤ 2θ ≤ 85° and in steps of 0.02° using a DX-2700 X-ray diffractometer (Dandong Haoyuan). Lattice parameters and unit cell volume were calculated by MS Modeling software package (Accelrys) using Rietveld refinement in Reflex Package and Cu Kα1 radiation (λ = 1.540562 Å). Scanning electric microscopy (SEM) (Zeiss) investigation in backscattered electron (BSE) mode was performed to detect potential secondary phase. PL of ceramic powders were measured at room temperature using a LabRAM XploRA Raman spectrometer (Horiba Jobin Yvon), with a 638-nm excitation wavelength. The laser power level was limited to 1 % of the normal output of 25 mW.

3. RESULTS AND DISCUSSION

3.1 Crystalline Structure and Microstructure

The powder XRD pattern of BNTH4 is shown in Figure 1. BNTH4 exhibited a single-phase cubic perovskite structure, as marked by a symmetric (200) characteristic peak. The Miller indexes are given in this figure. The unit-cell volume (V_0) of BNTH4 was calculated to be 64.68 Å^3.

BSE was used to detect potential secondary phases. The BSE image of the polished and thermally etched surfaces of BNTH4 is shown in Figure 2. No secondary phase was observed, which is in agreement with the above XRD result. Both XRD and BSE results reveal that Nd^{3+} and Ho^{3+} ions were completely incorporated into the $BaTiO_3$ host lattice.

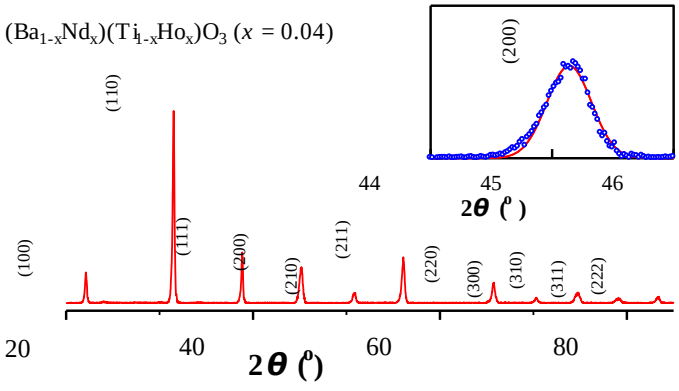

Figure 1: Powder XRD pattern of BNTH4. The inset shows Gaussian fitting of the XRD peak in the vicinity of 45°.

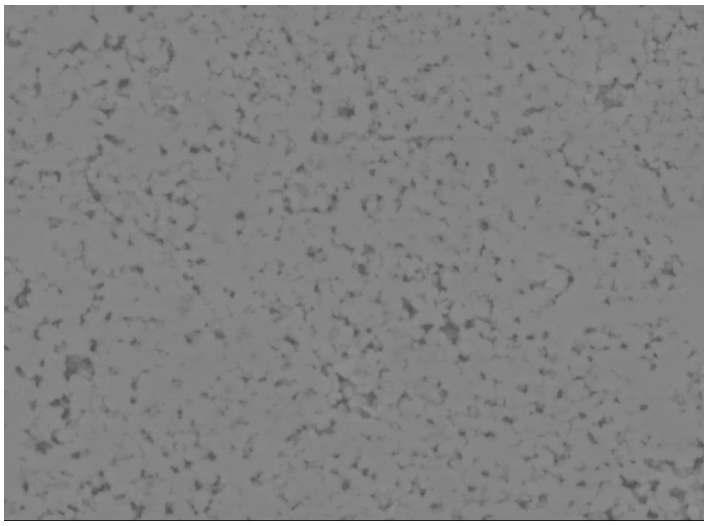

Figure 2: BSE image of the polished and thermally etched surface of BNTH4.

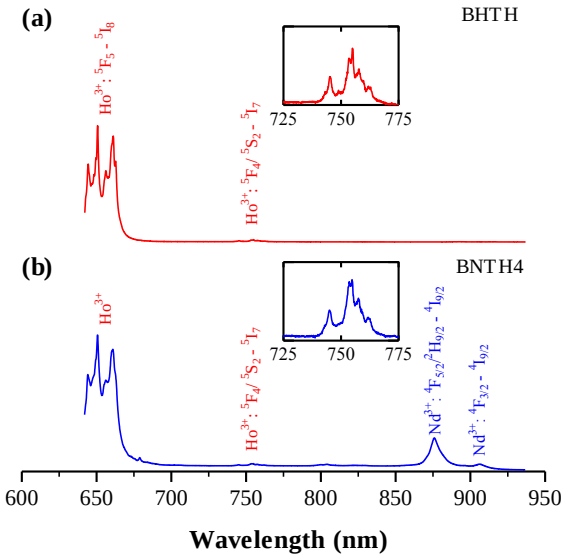

Figure 3: PL spectra of (a) BHTH, and (b) BNTH4 ceramics. Excitation: 638-nm laser line [18]. The two insets show enlarged peak bands at around 750 nm for BHTH and BNTH4.

3.2 PL INVESTIGATIONS

The PL spectra under 638-nm excitation for $(Ba_{1-x}Ho_{3x/4})(Ti_{1-x}Ho_{x/4})O_3$ (x = 0.01) (BHTH), and BNTH4 ceramics are shown in Figure 3 [18]. The enlarged peak bands at around 750 nm for BHTH and BNTH4 are shown in two insets in Figure 3. The PL signals from Ho^{3+} ions in BNTH4 were so intense that they concealed the traditional Raman spectra of $BaTiO_3$. Upon 638-nm excitation, two PL bands of around 653 and 755 nm wavelength appeared in the spectrum of BNTH4 (Figure 3b), originating from $^5F_5 \rightarrow ^5I_8$ and $^5F_4/^5S_2 \rightarrow ^5I_7$ transitions of Ho^{3+}, respectively, as observed in Figure 3a; two additional PL bands at 804 and 875 nm correlated to PL of Nd^{3+} (Figure 3b), which are attributed to $^4F_{5/2} \rightarrow ^4I_{9/2}$ and $^4F_{3/2} \rightarrow ^4I_{9/2}$ transitions of Nd^{3+} [13,17–21].

The energy level diagram for Ho^{3+} and Nd^{3+} ions in BNTH4 is shown in Figure 4. No evident energy transfer and down-conversion luminescence between Ho^{3+} and Nd^{3+} occurred under 638-nm excitation. The emission mechanism of Nd^{3+} ions in BNTH4 is as follows: Nd^{3+} ions are excited through one-photon absorption from the ground state $^4I_{9/2}$ to the excited state $^4F_{9/2}$ that relaxes non-radiatively to the lying excited state $^4F_{5/2}/^4H_{9/2}$ *via* continuous multi-phonon relaxation processes ($^4F_{9/2}$-$^4F_{7/2}/^4S_{3/2}$-$^4F_{5/2}/^2H_{9/2}$). Finally, the transitions of $^4F_{5/2} \rightarrow ^4I_{9/2}$ and $^4F_{3/2} \rightarrow ^4I_{9/2}$ occurred at 804 and 875 nm.

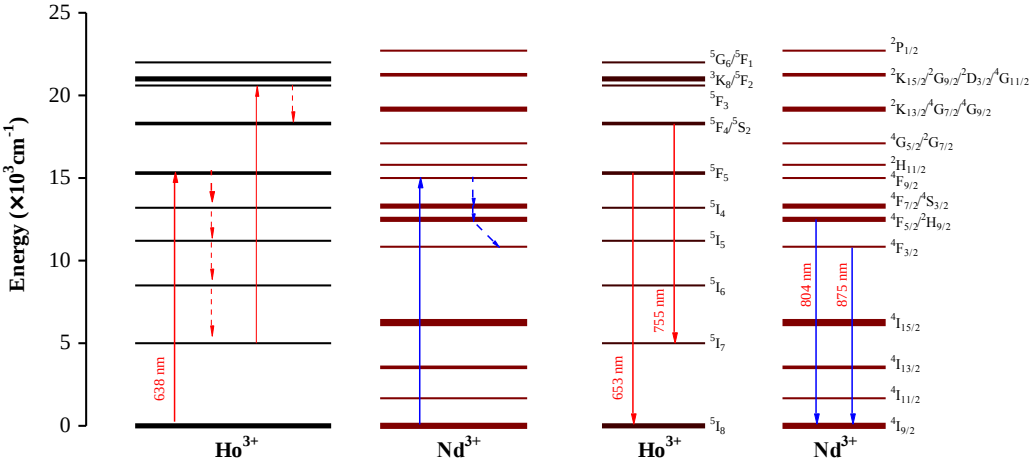

Figure 4: Energy level diagram for Ho3+ and Nd3+ ions in BNTH.

3.3 Ba-Site Occupancy of Ho^{3+} in BNTH4

It was reported that 0.75 at. % Ho^{3+} ions substituted at Ba-sites and 0.25 at.% Ho^{3+} ions substituted at Ti-sites in BHTH sintered at T_s = 1400 °C, and these two peaks at ~653 nm and ~755 nm in Figure 3 a arise from Ba-site Ho^{3+} [18]. They also appeared in the spectrum of BNTH4, which gives the evidence of some Ho^{3+} ions at Ba-sites in BNTH4. That is to say, Ho^{3+} ions dominantly occupy Ti-sites and a certain amount of Ho^{3+} ions occupy Ba-sites in BNTH4; Ho^{3+} exhibits an amphoteric behavior. On the basis of comparison in PL intensity between BNTH4 to BHTH, it is inferred that 0.18 and 3.82 at.% Ho^{3+} ions were substituted respectively for Ba-sites and Ti-sites in BNTH4.

4. CONCLUSION

BNTH4 ceramic was prepared using the cold-pressing ceramic technique. BNTH4 has a cubic perovskite structure. Upon excitation with 638-nm laser line, the PL monitoring provided the evidence of Ho^{3+} at Ba-site in BNTH4 and BNTH4 exhibits the multiplicity of signals of Nd^{3+}/Ho^{3+}. Ho^{3+} in BNTH4 exhibits an amphoteric behavior, i.e., 3.82 at.% Ho^{3+} ions dominantly occupy Ti-sites and 0.18 at.% Ho^{3+} ions occupy Ba-sites.

Cite The Article: Dongxue Guan, Dayong Lu, Xiuyun Sun (2018). Photoluminescence Of $(Ba_{0.96}nd_{0.04})$ $(Ti_{0.96}ho_{0.04})$ O_3 Ceramic Under 638-Nm Excitation. *Topics in Chemical & Material Engineering*, 1(1) : 101-103.

ACKNOWLEDGMENTS

This work was supported by the projects of the National Natural Science Foundations of China (Grant No. 21271084) and of Jilin Province (20160101290JC), Changbai Mountain Scholar Distinguished Professor (2015047), and Key Laboratory of Functional Materials Physics and Chemistry of the Ministry of Education (Jilin Normal University, China) (2016001).

REFERENCE

[1] Lu, D., Sugano, M., Toda, M. 2006. High-permittivity double rare-earth-doped barium titanate ceramics with diffuse phase transition, Journal of American Ceramic Society, 89, 8112–8123.

[2] Meneses-Nava, M.A., Barbosa-García, O., Maldonado, J.L., Ramos-Ortíz, G., Pichardo, J.L., Torres-Cisneros, M., García-Hernández, M., García-Murillo, A., Carrillo-Romo, F.J. 2008. Yb^{3+} quenching effects in co-doped polycrystalline $BaTiO_3$: Er^{3+}, Yb^{3+}, Optical Materials, 31, 252–260.

[3] Liu, Y., Pisarski, W.A., Zeng, S., Xu, C., Yang, Q. 2009. Tri-color upconversion luminescence of rare earth doped $BaTiO_3$ nanocrystals and lowered color separation, Optical Express, 17, 2301–2308.

[4] Ferreira, E.A., Cassanjes, F.C., Poirier, G. 2013. Crystallization behavior of a barium titanate tellurite glass doped with Eu^{3+} and Er^{3+}, Optical Materials, 35, 1141–1145.

[5] Dutta, D.P., Ballal, A., Nuwad, J., Tyagi, A.K. 2014. Optical properties of sonochemically synthesized rare earth ions doped $BaTiO_3$ nanophosphors: Probable candidate for white light emission, Journal of Luminescence, 148, 230–237.

[6] Gomes, M.A., Lima, A.S., Eguiluz, K.B., Salazar-Banda, G.R. 2016. Wet chemical synthesis of rare earth-doped barium titanate nanoparticles, Journal of Materials Science, 51, 4709–4727.

[7] Tang, B., Zhang, S., Zhou, X. 2009. The effects of Gd/Nd co-doping on the microstructure and dielectric properties of $BaTiO_3$ ceramics, Jppanese Journal of Applied Physics, 48, 111402.

[8] Kim, J., Kim, D., Kim, J., Kim, Y., Hui, K.N., Lee, H. 2011. Selective substitution and tetragonality by co-doping of dysprosium and thulium on dielectric properties of barium titanate ceramics, Electronic Materials Letters, 7, 155–159.

[9] Kim, D., Kim, J., Noh, T., Ryu, J., Kim, Y., Lee, H. 2012. Dielectric properties and temperature stability of $BaTiO_3$ co-doped La_2O_3 and Tm_2O_3, Current Applied Physics, 12, 952–956.

[10] Kim, J., Lee, H. 2013. Substitutional analysis of perovskite-type dysprosium and thulium co-doped barium titanate ceramics by a near edge X-ray absorption fine structure, Materials Letters, 92, 39–41.

[11] Gong, H., Wang, X., Zhang, S., Li, L. 2016. Synergistic effect of rare-earth elements on the dielectric properties and reliability of $BaTiO_3$-based ceramics for multilayer ceramic capacitors, Materials Research Bullstin, 73, 233–239.

[12] Cui, S., Lu, D. 2015. Study on solubility of La^{3+}-Dy^{3+} defect complexes and dielectric properties of $(Ba_{1-x}La_x)(Ti_{1-x}Dy_x)O_3$ ceramics, Ceramics International, 41 (2), 2301–2308.

[13] Pazik, R., Hreniak, D., Strek, W. 2004. Synthesis and luminescence properties of nanocrystalline $BaTiO_3$: Nd^{3+} obtained by sol-gel methods, Materials Science-Poland, 22, 219–225.

[14] Darwish, A.G.A., Badr, Y., Shaarawy, M.E., Shash, N.M.H., Battisha, I.K. 2010. Influence of the Nd^{3+} ions content on the FTIR and the visible up-conversion luminescence properties of nano-structure $BaTiO_3$, prepared by sol–gel technique, Journal of Alloys and Compounds, 489, 451–455.

[15] Battisha, I.K. 2004. Visible up-conversion luminescence in Ho^{3+}: $BaTiO_3$ nano-crystals prepared by sol gel technique. Journal of Sol-Gel Science and Technology, 30, 163–172.

[16] Secu, M., Cernea, M., Secu, C.E., Vasile, B.S. 2011. Structural characterization and photoluminescence of nanocrystalline Ho-doped $BaTiO_3$ derived from sol–gel method. Journal of Nanoparticle Research, 13, 3123–3128.

[17] Lu, D., Guan, D., Li, H. 2018. Multiplicity of photoluminescence in Raman spectroscopy and defect chemistry of $(Ba_{1-x}R_x)(Ti_{1-x}Ho_x)O_3$ (R = La, Pr, Nd, Sm) dielectric ceramics, Ceramics International, 44, 1483–1492.

[18] Lu, D., Guan, D. 2017. Photoluminescence associated with the site occupations of Ho^{3+} ions in $BaTiO_3$, Scientific Reports, 7, 6125.

[19] Pokhrel, M., Ray, N., Kumar, G.A., Sardar, D.K. 2012. Comparative studies of the spectroscopic properties of Nd^{3+}: YAG nanocrystals, transparent ceramic and single crystal, Optical Materials Expxpress, 2, 235–249.

[20] Beeby, A., Faulkner, S. 1997. Luminescence from neodymium(Ш) in solution, Chemical Physics Letters, 266, 116–122.

[21] Metcalfe, G.D., Readinger, E.D., Enck, R., Shen, H., Wraback, M., Woodward, N.T., Poplawsky, J., Dierolf, V. 2011. Near-infrared photoluminescence properties of neodymium in in situ doped AlN grown using plasma-assisted molecular beam epitaxy, Optical Materials Expxpress, 1, 84–90.

ABOUT THE AUTHORS

Professor Dayong Lu was born on July 31, 1967, in Liaoning, China. He earned a bachelor's degree in 1989 and a master's degree in 1996 from Jilin University and a PhD from Yamagata University in 2005. He taught at Jilin Institute of Chemical Technology (JLICT) in China. His research areas are high-permittivity ceramic materials, pharmaceutical analysis and quality control of traditional Chinese medicines, temperature-dependent measuring technology, and inorganic-organic composite materials. He is President of College of Materials Sciences and Engineering, Academic Leader of Materials Science and Engineering discipline, JLICT, Director of Key Laboratory of Special Functional Materials in Jilin Provincial Colleges and Universities. He was awarded New Century Excellent Talents in University, State Education Ministry (2007); Changbai Mountain Scholar Distinguished Professor (2016); and State Department Special Allowance (2015).

Dongxue Guan was born on January 15, 1990, in Jilin, China. She earned a bachelor's degree from Jilin Institute of Chemical Technology in 2014. She is a postgraduate in Jilin Institute of Chemical Technology. Her research area is high-permittivity ceramic materials.

Professor Xiuyun Sun was born on May 25, 1967, in Heilongjiang, China. She earned a bachelor's degree in 1989 and a PhD in 1999 from Jilin University. She taught at Jilin Institute of Chemical Technology (JLICT) in China. Her research areas are high-permittivity ceramic materials and Physical Chemistry.